Smooth Delaunay–Voronoï Dual Meshes for Co-Volume Integration Schemes

Igor Sazonov, Oubay Hassan, Kenneth Morgan and Nigel P.Weatherill

Civil & Computational Engineering Centre, University of Wales Swansea,
Singleton Park, Swansea, SA2 8PP, U.K.
`i.sazonov@swansea.ac.uk`

1 Introduction

Yee's scheme for the solution of the Maxwell equations [1] and the MAC algorithm for the solution of the Navier–Stokes equations [2] are examples of co-volume solution techniques. Co-volume methods, which are staggered in both time and space, exhibit a high degree of computationally efficiency, in terms of both CPU and memory requirements compared to, for example, a finite element time domain method (FETD). The co-volume method for electromagnetic (EM) waves has the additional advantage of preserving the energy and, hence, maintaining the amplitude of plane waves. It also better approximates the field near sharp edges, vertices and wire structures, without the need to reduce the element size. Initially proposed for structured grids, Yee's scheme can be generalized for unstructured meshes and this will enable its application to industrially complex geometries [3].

Despite the fact that real progress has been achieved in unstructured mesh generation methods since late 80s, co-volume schemes have not generally proved to be effective for simulations involving domains of complex shape. This is due to the difficulties encountered when attempting to generate the high quality meshes that satisfying the mesh requirements necessary for co-volume methods. In this work, we concentrate on EM wave scattering simulations and identify the necessary mesh criteria required for a co-volume scheme. We also describe several approaches for generating two-dimensional and three-dimensional meshes satisfying these criteria. Numerical examples on the scattering of EM waves show the efficiency and accuracy that can be achieved with a co-volume method utilising the proposed meshing scheme.

2 Mesh Requirements

For co-volume integration schemes to be implemented on unstructured meshes, the triangulation has to satisfy a number of criteria. For EM simulations, since

the schemes are staggered in space, co-volume methods need two mutually orthogonal meshes for the electric and magnetic fields. The dual Delaunay–Voronoï diagram is the obvious choice. In 2D, corresponding edges of the Voronoï and Delaunay meshes are mutually orthogonal. In 3D, every edge of the Voronoï diagram is orthogonal to the corresponding face of the Delaunay triangulation and vice versa.

Both meshes must be sufficiently smooth, i.e. the edges in both meshes must not be too short or too long. The stability property of an explicit implementation determines the time step in terms of the shortest edge in both meshes. Thus, all the edges should have length $\mathcal{O}(\delta)$, where δ is the recommended element size based upon the characteristic wavelength, λ, of the problem. The typical value used in many simulations is $\delta = \lambda/15$.

In addition, from the view point of accuracy, the Delaunay mesh should not contain bad elements, where, in this context, an element is defined as bad if its circumcentre is located outside the element.

A brief explanation of the main requirements can be found in the Appendix.

3 Mesh Quality Criteria

The criteria employed to determine the suitability of the mesh have to reflect the requirements of the numerical solution procedure. The simple formula

$$Q = \beta \frac{\min\{l_D, l_V\}}{\langle l_D \rangle} \tag{1}$$

is very useful to estimate the quality of the mesh built for wave scattering purposes. Here, $\beta = \sqrt{8}$ is a normalization coefficient, which gives $Q = 1$ for an ideal mesh (see Section 5), l_D is the Delaunay edge length, l_V is the Voronoï edge length and $\langle l_D \rangle$ is the average Delaunay edge length. The minimum is taken over all sides of both meshes.

If the mesh contains some bad elements, then the fraction,

$$r_{\text{bad}} = \frac{N_e^{\text{bad}}}{N_e}, \tag{2}$$

is also a criterion which may be used to compare different meshes. Here N_e is the total number of elements in the mesh and N_e^{bad} is the number of bad elements.

A sufficient condition to ensure the smoothness of the Voronoï diagram, is to ensure that every element has its circumcentre inside the element and located as far as possible from its edges or faces. In this case, the measure

$$q_e = 3 \frac{h_e}{R_e} \equiv 3 \cos \left(\max_{i=1,\ldots,4} \alpha_i \right) \tag{3}$$

is employed to estimate the quality of each individual element. In this expression, R_e is the circumradius, $h_e = \min\limits_{i=1,\ldots,4} h_i^e$ is the signed shortest distance from the circumcentre to an element edge or face (set negative if the circumcentre lies outside the element). For a perfect tetrahedral element $q_e = 1$; $q_e < 0$ for a bad element. This quality parameter q_e is also related to the maximal vertex angle α_i of an element. In 2D the vertex angle is simply the angle between the two edges connected to this vertex. In 3D the analogous tetrahedron vertex angle has a more complicated definition. The angle α_i of vertex P_i is defined as the angle under which a circumcircle of the face op-
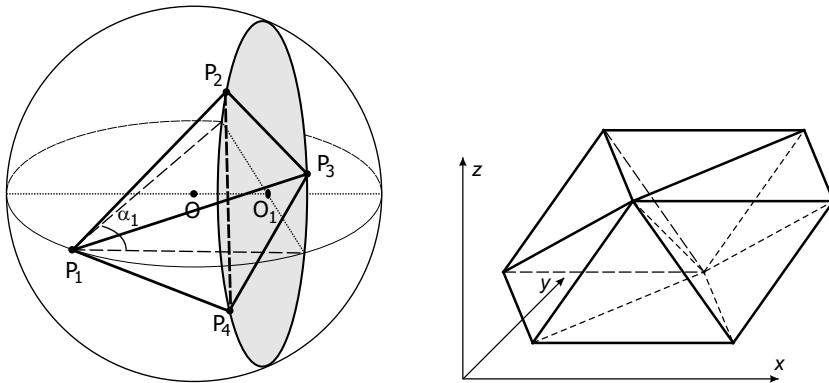

Fig. 1. On the definition of 3D element angle (left). Six elements of 3D ideal mesh form a parallelepiped tiling the space (right).

posite to P_i is seen from P_i in the plane passing through P_i and centre of element's circumsphere, O, and face's circumcircle, O_i, as seen in figure 1. The segment OO_i has length h_i. A good quality element, with $q_e > 0$, will have all acute vertex angles. It can be shown that, if $q_e > 0$ for all elements of the mesh, then the mesh is guaranteed to be Delaunay satisfying [4].

It can be shown that the necessary condition to ensure a good quality tetrahedral element, $q_e > 0$, with circumcentre located inside the element, is that the four triangular faces of the element should have acute angles [4]. Therefore, it is important to ensure that the initial boundary triangulation consists of triangles with all acute angles.

If all the tetrahedron vertex angles defined above are acute, some dihedral angles can be right or obtuse. A tetrahedron with all acute dihedral angles can have its circumecentre located outside its volume and hence can have an obtuse vertex angle.

Notice also, that although the tetrahedron vertex angle and the solid angle for the same vertex are not related uniquely, nevertheless the solid angle is

less/equal/greater than 2π, if the vertex angle is acute/right/obtuse, respectively.

4 Traditional Meshing Methods

Traditional unstructured mesh generation methods, such as the advancing front technique (AFT) [5] and the Delaunay triangulation [6], as well as their combinations [7], are not designed to guarantee the creation of a mesh meeting the requirements set out above, even in the two-dimensional case. These methods generate meshes in which the element edge length is normally acceptable, but the corresponding Voronoï diagram may often be highly irregular, with some very short Voronoï edges. Thus, these methods cannot guarantee the regularity of the edge lengths of the dual mesh and the absence of bad elements, even in 2D. Mesh improvement methods, based on swapping, reconnection [8] and smoothing, improve the quality of 2D meshes. Nevertheless, a significant number of very short Voronoï edges and bad elements, located mainly near the domain boundary, remain in the final mesh [9]. In 3D, the advancing front technique (AFT) can produce meshes with about 60% of bad elements and these are unsuitable for a co-volume solution scheme.

A promising approach is the construction of the centroidal Voronoï tessellation (CVT) and its dual Delaunay mesh. The CVT relocates the generated nodes to be at the mass centroids of the corresponding Voronoï cells with respect to a given density function [10]. A new Voronoï tessellation of the relocated nodes is produced. This process, which is called Lloyd's algorithm [11], can be repeated until all nodes are close enough to the corresponding centroids. Lloyd's algorithm needs an initial mesh, which can be generated by any method. In addition to relocating the nodes, the CVT scheme changes the mesh topology. Although the quality of final mesh is much higher than the quality of the initial mesh, it is normally not suitable for the successful application of co-volume solution schemes: in 3D, the share of bad elements is usually around 10% of the total elements, although this can be reduced to 3–5% for specially prepared initial meshes.

An alternative approach is the stitching method [9]. In this approach, the problem of triangulation is split into a set of relatively simple problems of local triangulation. Firstly, in the vicinity of boundaries, body fitted local meshes are built with properties close to those regarded as being ideal. An ideal mesh is employed, away from boundaries, to fill the remaining part of the domain. These mesh fragments are then combined, to form a consistent mesh, with the outer layer of the near boundary elements stitched to a region of ideal mesh by a special procedure, in which the high compliance of mesh fragments is used. This will result in high quality meshes compared to those built by other methods [9].

5 Ideal Mesh

In 2D, a mesh of equilateral triangles is an ideal mesh. The index of every node, i.e. the number of nodes connected to a node, is 6, the Voronoï edge length $l_V = l_D/\sqrt{3} \approx 0.56\,l_D$, the element quality is $q_e = 1$ and all the vertex angles are $60°$. A 3D analogue of this ideal mesh consists of equal non-perfect tetrahedra, each face of which is an isosceles triangle with one side of length l_D^{long} and two shorter sides of length $l_D^{\text{short}} = (\sqrt{3}/2)\,l_D^{\text{long}}$. Six such tetrahedra form a parallelepiped tiling the space, as illustrated in Figure 1. It can be shown that this configuration maximises the minimum Voronoï edge for a fixed element size. All Voronoï edges have the same length $l_V \approx 0.38\,\delta$ where $\delta \equiv \langle l_D \rangle = (3\,l_D^{\text{long}} + 4\,l_D^{\text{short}})/7 \approx 0.92\,l_D^{\text{long}}$. This configuration guarantees that the element quality is $q_e \approx 0.95$ and that every node has an index of 14. All vertices have an acute angle, $71.5°$, and hence, the circumcentre is located inside each element. However, certain dihedral angles are equal to $90°$, which is larger than the value $\alpha = \arccos(1/3) = 70.5°$ for the perfect tetrahedron. The 2D and 3D ideal meshes satisfy the requirements listed in Section 2, but do not necessarily fit the boundaries of an arbitrary domain to be triangulated.

6 Near Boundary Triangulation

If the domain boundary is smooth enough i.e. if its radius of curvature is much greater than δ, then building the first few layers of a body fitted mesh is an elementary task in 2D: the near boundary mesh has the same topology as the 2D ideal mesh. A well tuned 2D advancing front method is capable of producing a high quality near boundary mesh of this type. Modifications to the method, which improve the mesh quality if the boundary curvature is not small, are described in [9].

The analogous 3D problem is not elementary, even for the problem of generating high quality tetrahedral elements near a plane boundary discretised with a 2D ideal mesh. Using the 3D advancing front technique, which is regarded to be an effective method for placing points, we can build a perfect tetrahedron on every boundary triangle (Figure 2a). The first layer of new points forms a hexagonal structure which cannot be connected to form triangles which are all acute. This is illustrated in Figure 3. Hence, this method applied directly, which generating nearly twice the number of boundary points, cannot even produce a mesh of the desired form for the first layer.

Analyzing the structure of the 3D ideal mesh, it can be concluded that the best location of a new point is above the edge shared by two conjugate surface triangles (Figure 2b). Starting from a plane boundary with an ideal 2D triangulation, the boundary triangles are grouped into pairs sharing the same edge. A New points are located above these edges. The optimal position for the points is at a distance of 0.684 of the boundary edge length from the
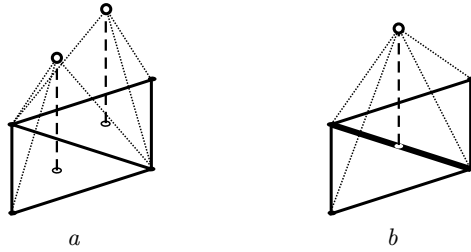
Fig. 2. (a) Placing a new point above centroid of boundary triangles as in classical AFT. (b) Placing a new point above a midpoint of an edge (bold line) shared by two boundary triangles. Open circles indicate new points, dotted lines show new edges of formed nearly boundary tetrahedra.
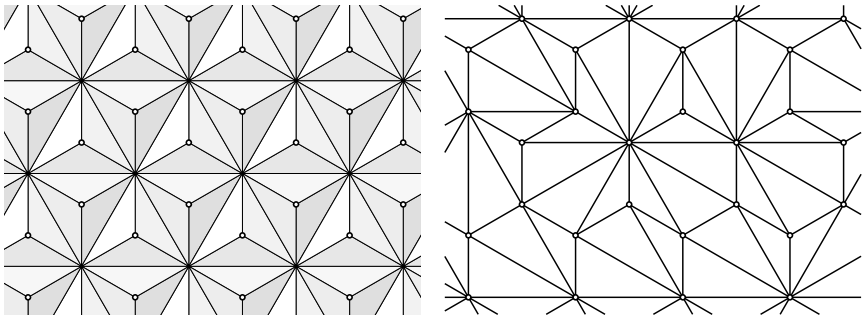

Fig. 3. Perfect tetrahedra built at every boundary triangle (view from above the boundary) (left). Delaunay connection of their apexes (right)

plane. This minimises the worst element quality at $q_e = 0.795$. This procedure ensures that the number of new points similar to that of the initial boundary points. This means that the triangulation can be continued layer by layer to form a 3D mesh with the same topology as the 3D ideal mesh. This process is demonstrated in Figure 4.

In the general case, the boundary triangulation does not have the topology of 2D ideal mesh on a plane with all nodal indexes equal to 6. Therefore, when we group all the boundary faces into pairs, some of the generated triangles will remain ungrouped (Figure 5). For such an ungrouped triangle, point in the next layer must be located above its circumcentre, as in the standard advancing front technique. If the topology of the boundary mesh is good enough, i.e. if the index of most nodes is 6, and a relatively small number of nodes have index 5 and 7, then the number of uncoupled triangles is relatively small. Hence, the number of points in the the next layer will only slightly exceed the number of boundary points. All the points are connected by the Delaunay method and a new layer is formed. This can be viewed as a sophisticated
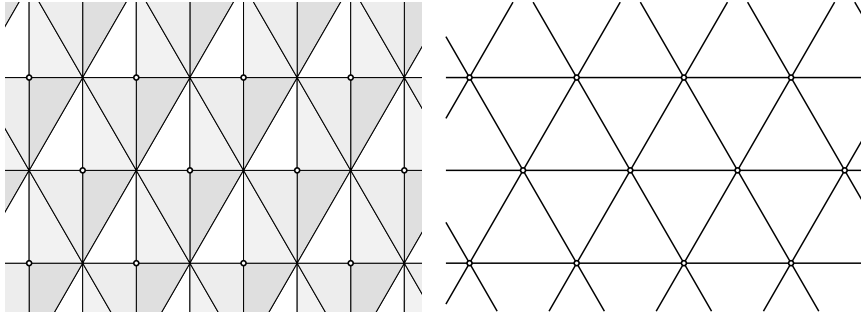
Fig. 4. Tetrahedra built if nodes are placed above edges (left). Boundary triangulation (solid) and Delaunay connection of nodes (dashed) (right).
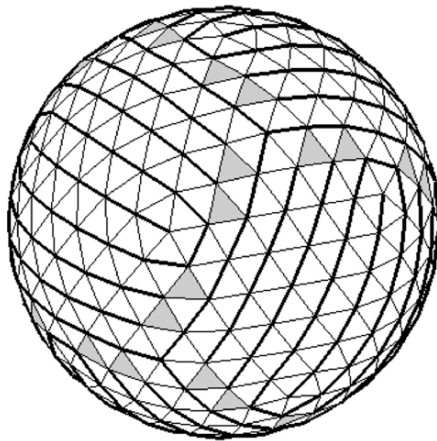

Fig. 5. Set of boundary faces is split by non-intersecting pairs of triangles sharing this same edge. Those edges are indicated by a bold lines. Non-coupled triangles are indicated by grey.

version of the 3D advancing front method for placing points, coupled with the Delaunay method for connecting points.

An example of a mesh produced by the basic AFT for a domain with a slightly curved boundary, and with a nearly ideal boundary mesh, is shown in Figure 6. Here only tetrahedra having boundary faces are shown. The colour indicates the tetrahedron quality: with white to red corresponding to quality q_e from 1 to zero and from blue to black corresponds to the quality q_e from zero to -3. It can be observed that a significant number of bad elements remains.

Figure 7 shows several views of the first layer of a mesh generated using the proposed method. The colour–quality indication is the same as that used in
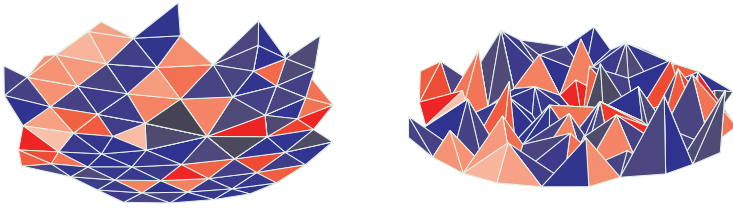
Fig. 6. Fragment of triangulation by the classical AFT. Elements having boundary face are shown only. View from the outside (left) and from the domain (right).

Figure 6. It should be noted that the near boundary triangulation is the most demanding part of the stitching method. Furthermore, acute near boundary triangulation will automatically solve the problem of boundary recovery, which is an essential part of any Delaunay triangulation.
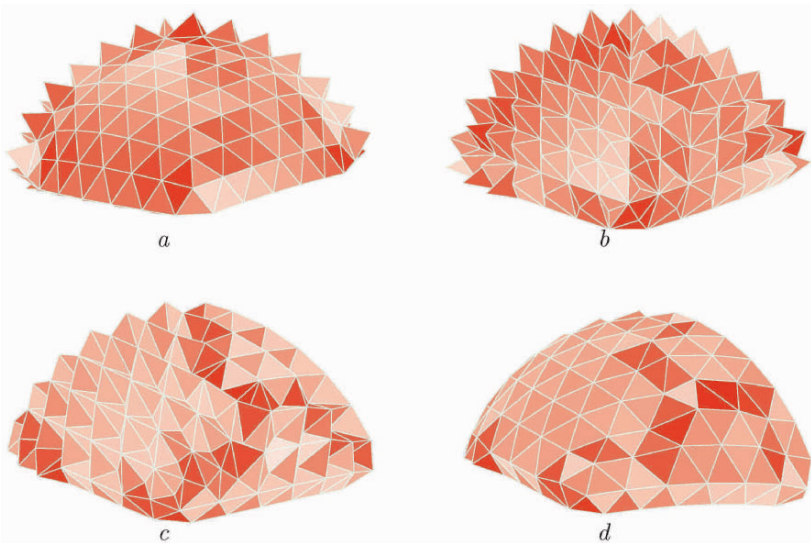

Fig. 7. Fragment of the triangulation by the new method. View from the outside (*a*) and from the domain (*b–c*), elements having boundary face (*a,b*), also elements having boundary edge (*c*), also elements having boundary node (*d*)

Steps in creating a new layer:

1. Split all boundary (or frontal) triangles by pair of triangles sharing the same edge, minimizing the number of single triangles.
2. Locate new points above midpoint of the shared edges and above centroid of single triangle.
3. Connect all the points by Delaunay method.

7 Example of a Domain Triangulation.

A simple domain, made of two spherical surfaces, is triangulated using the procedure described above. The size of elements used increases towards the outer sphere. A cut through the triangulation is shown in Figure 8. The colour–quality indication is the same as in Figures 6 and 7. The mesh contains some bad elements, with $q_e \approx -0.017$, but they form just 0.12% of the elements only, i.e. 256 among $N_e = 218,816$. The shortest Voronoï edge is $0.05\,\delta$, 87% of the internal nodes have the ideal index of 14, and the rest of the nodes have indices between 10 and 16. To compare the quality of the generated mesh with that obtained by other methods, the same 3D domain and the same boundary triangulation were used to generate meshes using an advancing front method, a Delaunay triangulation and a coupled Delaunay and CVT scheme. Various mesh quality criteria were computed: the global quality criteria, Q defined in equation (1); the percentage of bad elements in the mesh r_{bad}; the individual

Table 1. Comparison for different meshing methods

Method	Q	r_{bad}	q_e		$3R_e^{\mathrm{in}}/R_e$		nodal index	
			min	mean	min	mean	min	max
Advancing Front	$4 \cdot 10^{-7}$	67%	-3	-0.49	$3 \cdot 10^{-4}$	0.65	4	37
Delaunay	$2.4 \cdot 10^{-6}$	50%	-2.2	-0.07	$5 \cdot 10^{-3}$	0.72	8	24
Delaunay+CVT	$1.0 \cdot 10^{-5}$	9.8%	-1.2	0.39	0.08	0.88	9	21
Present method	$4.8 \cdot 10^{-2}$	0.12%	-0.02	0.65	0.74	0.92	10	16

element quality q_e, defined in equation (3); a standard criterion of the ratio an element's inradius R_e^{in} to its circumradius. To estimate topological properties of the obtained meshes, the range of the nodal index for internal nodes was also determined. The results are displayed in Table 1. It can be seen that the new method gives much improved mesh quality compared to all other methods.
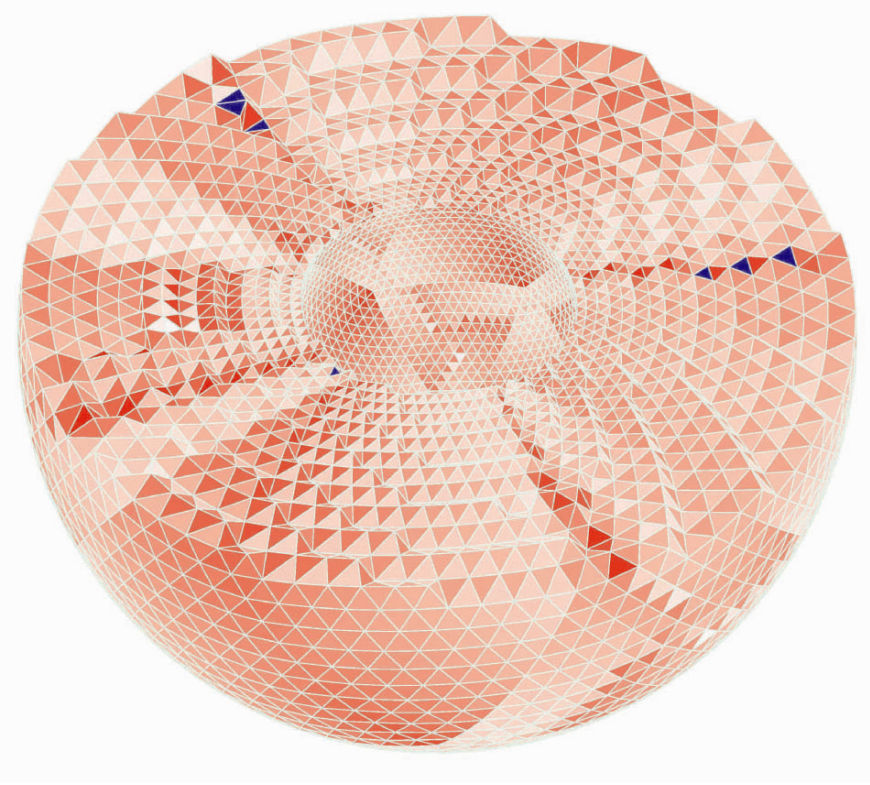
Fig. 8. Cut of the triangulation of a spherical layer.

8 Numerical Results

This mesh has been used with a co-volume integration scheme for Maxwell's equations. The unknowns are the projections of the electric field onto the Delaunay edges and the projections of the magnetic field onto the Voronoï edges. The solution is advanced in time using a staggered explicit scheme. The wave frequency is such that the diameter of the sphere is 2λ. The size of the elements near the scattering PEC sphere is approximately $\lambda/15$. Near the external boundary, the element size is $\lambda/6$. The distance between the boundaries is large enough to neglect the reflection of wave from the external boundary during first three cycles. The number of time steps per cycle is 141. The computation time per time step is 0.1 s, which is ten times faster than the corresponding time for a conventional finite element time domain method on the same mesh. The computed radar cross section (RCS) distribution is
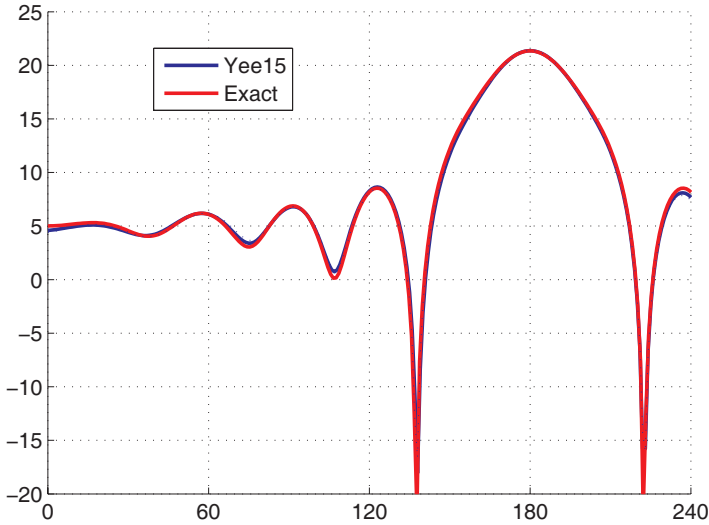
Fig. 9. Radar Cross Section exact (red) and computed by the co-volume method (blue).

compared with the exact distribution in Figure 9 and the maximum difference at any location is less than one tenth of a dB.

9 Conclusion

A new method of placing the points in 3D triangulation is proposed. The method produces a high quality near boundary triangulation. It has been demonstrated that the quality of the resulting mesh is such co-volume integration schemes can be successfully implemented. An example that demonstrates that the problem of building a mesh for a 3D domain for use with a co-volume solution scheme is solvable. Work on the generalization of the method for more complicated domains is currently in progress.

References

1. Yee K (1996) Numerical solution of initial boundary value problem involving Maxwell's equation in isotropic media, IEEE Trans Antennas and Propagation 14:302–307
2. Churbanov A (2001) An unified algorithm to predict compressible and incompressible flows. In: CD Proceedings of the ECCOMAS Computational Fluid Dynamics Conference, Swansea, Wales, UK

3. Morgan K, Hassan O, Peraire J (1996) A time domain unstructured grid approach to the simulation of electromagnetic scattering in piecewise homogeneous media, Computer Methods in Applied Mechanics and Engineering 134:17–36

4. Bern M, Chew L.P, Eppstein D, and Ruppert J (1995) Dihedral bounds for mesh generation in high dimensions. In: 6th ACM-SIAM Symposium on Discrete Algorithms, 189–196.

5. Peraire J, Vahdati M, Morgan K, Zienkiewicz O (1987) Adaptive remeshing for compressible flow computations, Journal of Computational Physics 72:449-466

6. George P, Borounchaki H (1998) Delaunay Triangulation and Meshing. Application to Finite Elements, Hermès, Paris

7. Marcum D, Weatherill N (1995) Aerospace applications of solution adaptive finite element analysis, Computer Aided Geometric Design, Elsevier, 12:709–731

8. Frey W, Field D (1991) Mesh relaxation: a new technique for improving triangulation, Int J Numer Meth in Engineering 31:1121–1133

9. Sazonov I, Wang D, Hassan O, Morgan K, Weatherill N (2006) A stitching method for the generation of unstructured meshes for use with co-volume solution techniques, Computer Methods in Applied Mechanics and Engineering 195/13-16:1826–1845

10. Du Q, Faber V, Gunzburger M (1999) Centroidal Voronoï Tessellations: Applications and Algorithms, SIAM Review 41/4:637–676

11. Lloyd S (1982) Least square quantization in PCM. IEEE Trans Infor Theory 28:129–137

12. Taflove A, Hagness S.C (2000) Computational electrodynamics: the finite–difference time domain method. 2nd ed., Artech House, Boston.

Appendix: Yee's scheme generalized to unstructured meshes

The Yee algorithm is based on: Ampere's law

$$\frac{\partial}{\partial t} \int_A \boldsymbol{E} \, d\boldsymbol{A} = \varepsilon \oint_{\partial A} \boldsymbol{H} \, d\boldsymbol{l} \tag{4}$$

and Faraday's law

$$\frac{\partial}{\partial t} \int_A \boldsymbol{H} \, d\boldsymbol{A} = -\mu \oint_{\partial A} \boldsymbol{E} \, d\boldsymbol{l} \tag{5}$$

applied to a surface A and its boundary ∂A. Here $\boldsymbol{E}$ and $\boldsymbol{H}$ are the electric and magnetic fields, respectively; $d\boldsymbol{A}$ is an element of surface area directed normal to the surface, $d\boldsymbol{l}$ is an element of the contour length directed tangent to the contour; ε and μ are the electric and magnetic permeability.

If a dual Delaunay–Voronoï diagram is built for the domain of integration, then equations (4) and (5) can be approximated as

$$\frac{E_i^n - E_i^{n-1}}{\Delta t} A_i^V = \varepsilon \sum_{k=1}^{M_i^V} H_{j_{i,k}}^{n+0.5} l_{j_{i,k}}^V, \quad i = 1, \dots, N_s^D \tag{6}$$

$$\frac{H_j^{n+0.5} - H_j^{n-0.5}}{\Delta t} A_j^D = -\mu \sum_{k=1}^{3} E_{i_{j,k}}^n l_{i_{j,k}}^D, \quad j = 1, \dots, N_s^V \qquad (7)$$

where E_i^n is the projection of the electric field onto the ith Delaunay side at the instant $n\Delta t$; $H_j^{n+0.5}$ is the projection of the magnetic field onto the jth Voronoï side at the instant $(n + 0.5)\Delta t$; l_i^D and A_i^V denote the length of the ith Delaunay side and the area of the corresponding Voronoï face respectively; l_j^V and A_j^D are the length of the jth Voronoï side and the area of the corresponding Delaunay face respectively; $j_{i,k}, k = 1, \dots, M_i^V$ are sides of a Voronoï face corresponding to the ith Delaunay edge (Figure 10a); $i_{j,k}, k = 1, 2, 3$ are sides of a Delaunay triangle face corresponding to the jth Voronoï edge (Figure 10b); N_s^D and N_s^e are the numbers of Delaunay and Voronoï sides in the mesh.
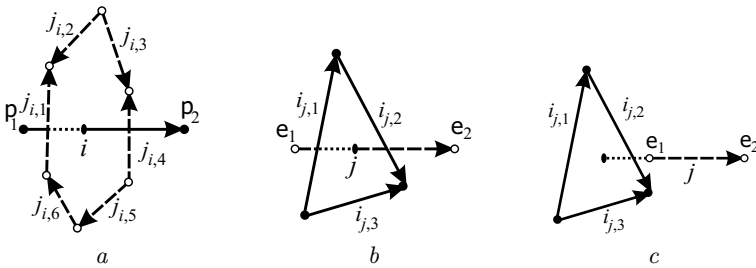

Fig. 10. The ith Delaunay side connecting nodes p_1-p_2 and correspondent Voronoï face formed by Voronoï sides $j_{i,1}, \dots, j_{i,6}$ (a). The jth Voronoï side connecting circumcentra of elements e_1-e_2 and correspondent Delaunay face formed by Delaunay sides $i_{j,1}, i_{j,2}, i_{j,3}$ (b-c). In (c) the Voronoï side does not intersect the correspondent Delaunay face.

Equations (6) and (7) form an explicit procedure for advancing the electric field form time t^n to $t^{(n+1)}$ and the magnetic field from time $t^{(n-0.5)}$ to $t^{(n+0.5)}$. For a structured grid this scheme is if $c\Delta t < l/\sqrt{3}$ where $c = 1/\sqrt{\varepsilon\mu}$ is the light speed, and l is an edge length. For an unstructured tetrahedral mesh, there is no such simple criterion but computations show that we can use the following relation

$$c\Delta t < S_f \min_{i,j}\{l_i^V, l_j^D\} \qquad (8)$$

where S_f is a safety factor.

In the co-volume scheme, the values of electric and magnetic field are taken at the intersection point of the edge and the correspondent face. If an element has its circumcentre outside its volume then the field will lie outside the edge connecting the two corresponding circumcentres (Figure 10c). In this case, the approximation of the integral cannot guarantee even the first order accuracy.